The projection effect on the measurement of the angular BAO scale

Edilson de Carvalho[1,2], Armando Bernui[1], Joel C. Carvalho[1]

[1]Observatório Nacional, 20921-400, Rio de Janeiro, RJ, Brazil;
[2]Centro de Estudos Superiores de Tabatinga, Universidade do Estado do Amazonas, 69640-000, Tabatinga, AM, Brazil

E-mail: dilsofilho@hotmail.com

Abstract. The baryon acoustic oscillations (BAO) imprinted a geometric spherical pattern in the distribution of cosmic structures, like quasars or galaxies. Such pattern can be detected by analyzing the 2-point correlation function of a large sample of cosmic objects, where it appears as a small excess of probability to find pairs of objects separated by a comoving distance: the radius of the sphere r_s. This signature appears in a 3-dimensional (3D) scrutiny, but also in the 2-dimensional (2D) study, with the data located in a thin redshift bin. Differently from the 3D case, in 2D analysis, the angular BAO scale is not directly obtained from the 2-point angular correlation function due to the projection effect, which arises because the size of the redshift bin is not null, and therefore a small shift-correction is needed. Here we estimate the magnitude of such shift-correction for several redshift epochs of the Universe, in the linear and nonlinear approaches.

1. Introduction

Modern cosmology has attained a high level of precision due to innovative and ambitious astronomical surveys [1,2]. With the huge amount of data publicly available, in several electromagnetic wavelenghts, cosmological models and parameters are being exhaustively tested [3,12]. We also learned to work with diverse observational probes to face on different astrophysical problems and paradigms.

The use of datasets to study the homogeneity and isotropy properties in the distribution of matter and radiation is an active field of research. But, we just have one observable Universe, therefore, the property of homogeneity, isotropy, or Gaussianity, can be investigated statistically, that is, as an average property with respect to simulated universes produced according to such hypotheses. Thus, the statistical isotropy feature has been examined with extra-galactic sources and probes like Radio-sources [13], Gamma-ray bursts [14], galaxy clusters [15], photometric galaxies from the WISE survey data [16], and also with the Planck convergence map κ [17]. In all these cases, the analyses show that the datasets are compatible with the statistical isotropy hypothesis. The cosmic microwave background (CMB) radiation is also consistent with statistical isotropy at small angles [18,19], although some controversy exists at the largest scales [20–24]. Another fundamental property of the CMB temperature fluctuations is their statistical distribution, extensively investigated in several analyses –employing diverse statistical tools–

that indicate just small deviations from the Gaussian hypothesis [18,25–27], studies that include non-primordial sources of non-Gaussianity, like residual foregrounds, the application of masks, and systematics [28–31].

The statistical homogeneity is a more delicate issue. Methods that intend to test the homogeneity of the matter distribution by counting objects in spheres or spherical caps (when the sources are projected on the sky) are not direct tests of spatial homogeneity, instead they can be considered as consistency tests of homogeneity [32-34].

Additionally, the large-scale structure and evolution of the Universe are being extensively studied, especially after the measurement, with good statistical significance, of the signature left by the baryon acoustic oscillations (BAO) [35]. The BAO is a primordial phenomenon that left imprinted a geometric spherical pattern in the distribution of luminous matter structures. Such pattern can be detected by analyzing the 2-point correlation function (2PCF) of a large sample of cosmic objects, like quasars or galaxies, where it appears as a small excess of probability to find pairs of objects separated by a comoving distance corresponding to the radius of the sphere, r_s. The fundamental importance of detecting and measuring this signature is because it defines a *cosmic distance ladder*, i.e., a scale to measure distances at any epoch of the Universe.

The information provided by this scale is being used to measure the dynamics of the Universe. This distance scale, r_s, is a signature found in 3-dimensional (3D) scrutinies using the 2PCF, but it is also present in the projected 2-dimensional (2D) analyses when the data is located in a thin redshift bin and is considered as projected on the celestial sphere (this means that we ignore their distance to us). In the 2D analysis, the angular BAO scale is obtained through the 2-point angular correlation function (2PACF), where the distances between pairs are obtained computing the angular separation between objects projected on the sky, analyses that do not assume a fiducial cosmological model. Differently from the 3D case, in 2D analysis the angular BAO scale is not directly obtained from the 2-point angular correlation function due to the projection effect, which arises because the redshift bin size is small but not null, and therefore a shift correction calculated using some fiducial cosmology is needed. This effect is smaller as thinner is the redshift bin where the 2D analysis is done. For this, one says that the measurement of the angular BAO scale in 2D is obtained in a quase model-independent approach. This quase model-independent method is an advantage in the task of determining the cosmological parameters. Here we estimate the size, in percent level, of such correction for several redshift bin sizes and in both linear and nonlinear approaches.

2. The 2-point angular correlation function

We aim is to measure the BAO angular scale, also termed the transversal BAO signal, for data in a redshift shell. The angular clustering of cosmic objects (like galaxies, quasars, or any cosmological tracer) located in a redshift shell can be investigated through the 2PACF [36–38]. Given a dataset of cosmic objects, the 2PACF is based on counting all pairs of cosmic objects $DD(\theta)$ at an angular separation θ, for $\theta \in [0°, \theta_{\rm max}]$, and compare this with the number of pairs $RR(\theta)$ from a similar count in a random catalogue (in practice one uses many random sets, see, e.g., ref. [39] for more details). The most used 2PACF estimator to compute the transversal BAO contribution, analysis that is done selecting the data sample in a sufficiently thin redshift shell δz, is the Landy-Szalay (LS) estimator [37], which returns the smallest deviations for a given cumulative probability, besides to have no bias and minimal variance (for alternative clustering analyses for large-scale structure in the Universe see, e.g., [40–42]). The expression

for the 2PACF estimator, $\omega(\theta)$ is given by

$$\omega(\theta) \equiv \frac{DD(\theta) - 2DR(\theta) + RR(\theta)}{RR(\theta)}\,, \tag{1}$$

where θ is the angular separation between any pair of cosmic objects [38,39].

The angular scale $\theta_{\rm FIT}$ of the BAO peak in the 2PACF can be found using the methodology proposed in Sánchez et al., 2011 [38] based on the empirical parametrization of $\omega = \omega(\theta)$,

$$\omega(\theta) = A + B\theta^{\gamma} + C\exp^{-(\theta-\theta_{\rm FIT})/2\sigma^2_{\rm FIT}}\,, \tag{2}$$

where A, B, C, γ, $\theta_{\rm FIT}$, and $\sigma_{\rm FIT}$ are free parameters. Then, the 2PACF best-fitting empirical expression (eq. 2) provides $\theta_{\rm FIT}$, while the width of the peak, $\sigma_{\rm FIT}$, defines the error associated to $\theta_{\rm FIT}$. The final measurement of the acoustic peak is achieved after accounting for an effect that produces a small shift of this BAO peak.

As a matter of fact, the finite thickness $\delta z \neq 0$ of the shell containing the data produces a shift in the acoustic peak due to a *projection effect*. To understand this effect consider first all objects on a spherical shell with radius equal to the characteristic BAO scale and centered on another object, therefore contributing to the BAO bump in a 3D analysis, where the central object is located at the redshift $\bar{z}$ (the mean value of the data in the redshift bin, of width δz, in study). In the case of the 2D analysis, the BAO signature in the 2PACF comes from the objects displayed along circles, or quasi circles, located in the transversal plane (the plane perpendicular to the line-of-sight). This means that, in the 2D analysis, one is assuming that all cosmic objects in the redshift bin are projected onto the sky patch with redshift $\bar{z}$. The effect produced on the BAO signature by this projection has been studied in detail (see, e.g., [28]) and the net result is a shift in the angular position of the BAO peak, which can be estimated using numerical analysis. In the following sections, we perform a detailed numerical analysis that calculates the shift for several epochs of the Universe (that is, calculation done considering the dataset at several redshifts).

2.1. The Projection Effect

To compute the projection effect for the case of data in a thin redshift bin $z \in [z_1, z_2]$, with mean $\bar{z}$, we first calculate the expected 2PCF, $\xi^{\bar{z}}_E$, assuming a fiducial cosmology

$$\xi^{\bar{z}}_E(s) = \int_0^{\infty} \frac{dk}{2\pi^2}\, k^2\, j_0(ks)\, P(k,\bar{z})\,, \tag{3}$$

where j_0 and $P(k,\bar{z})$ are the spherical Bessel function of zero order and the matter power spectrum for the assumed cosmological model, respectively.

Consider a sample of cosmic objects in a redshift bin $z \in [z_1, z_2]$, it is considered a thin bin because $z_1 \simeq z_2$. Due to this one has: $\xi^{z_1}_E(s) \simeq \xi^{z_2}_E(s) \simeq \xi^{\bar{z}}_E(s)$, where $\bar{z} \equiv (z_1 + z_2)/2$. Therefore, one can obtain the expected 2PACF, $\omega^{\bar{z}}_E(\theta)$, as a projection of the expected 2PCF, $\xi^{\bar{z}}_E(s)$, in that redshift shell by numerical integration

$$\omega^{\bar{z}}_E(\theta) = \int_0^{\infty} dz_1\, \phi(z_1) \int_0^{\infty} dz_2\, \phi(z_2)\, \xi^{\bar{z}}_E(s)\,, \tag{4}$$

where ϕ is the top-hat selection function which should be normalized to 1, s is the 3D separation between pairs; for a spatially flat Robertson-Walker metric s is obtained from:

$s = \sqrt{\zeta^2(z_1) + \zeta^2(z_2) - 2\zeta(z_1)\zeta(z_2)\cos\theta_{12}}$, where θ_{12} is the angular separation between the cosmic objects 1 and 2, and $\zeta(z_i)$ is the comoving radial distance to the cosmic object with redshift z_i, obtained using a cosmological model.

2.2. Numerical Analysis

To quantify the shift in the BAO bump due to the projection effect we compute the expected angular BAO scale, θ_E^0, which corresponds to the bump position when one computes the 2PACF using the equation (4) for the case of $\delta z = 0$. Next, one applies the same procedure but considering $\delta z = 0.05$, which is the thickness of the redshift shell used in the actual measurement, to find the expected the angular BAO scale $\theta_E^{\delta z}$. Then, the BAO angular scale at redshift $\bar{z}$, $\theta_{\rm BAO}(\bar{z})$, is given by

$$\theta_{\rm BAO}(\bar{z}) \,=\, \theta_{\rm FIT}(\bar{z})\,[1 \,+\, \Delta(\bar{z}, \delta z)]\,, \tag{5}$$

where

$$\Delta = \Delta(\bar{z}, \delta z) \equiv \frac{\theta_E^0 - \theta_E^{\delta z}}{\theta_E^0}\,, \tag{6}$$

is the relative difference between θ_E^0 and $\theta_E^{\delta z}$, and is used to perform the shift in the fitted value $\theta_{\rm FIT}(\bar{z})$ to finally obtain the measurement of the BAO angular scale $\theta_{\rm BAO}(\bar{z})$.

Our numerical analysis assumes six cosmological parameters: the baryon density $\omega_b \equiv \Omega_b h^2$, the cold dark matter density $\omega_c \equiv \Omega_c h^2$, the ratio between the sound horizon and the angular diameter distance to decoupling Θ, the optical depth to reionization τ, the overall normalization of the primordial power spectrum A_s, and the tilted scalar spectral index n_s. $H_0 = 100\,h\,km\,s^{-1}\,Mpc^{-1}$ is the Hubble constant, parametrized with the real number $h \in [0, 1]$. For the results shown in Table 1 we have considered the set of cosmological parameters obtained by the Planck collaboration [43].

Table 1. Values of the BAO bump position in the 2PACFs plotted in Figure 1. The relative difference, $\Delta = \Delta(\bar{z}, \delta z) \equiv (\theta_E^0 - \theta_E^{\delta z})/\theta_E^0$, for the linear (L) and non-linear (NL) cases.

	θ_E^0 ($\delta z = 0$)		$\theta_E^{\delta z}$ ($\delta z = 0.05$)			
z	L	NL	L	NL	Δ (L)	Δ (NL)
0.3	6.81°	6.71°	6.39°	6.32°	0.062	0.058
0.5	4.31°	4.21°	4.17°	4.09°	0.032	0.029
0.7	3.25°	3.22°	3.16°	3.11°	0.028	0.034
0.9	2.69°	2.66°	2.60°	2.56°	0.033	0.037
1.1	2.32°	2.30°	2.26°	2.24°	0.026	0.026
2.0	1.58°	1.57°	1.56°	1.55°	0.013	0.013

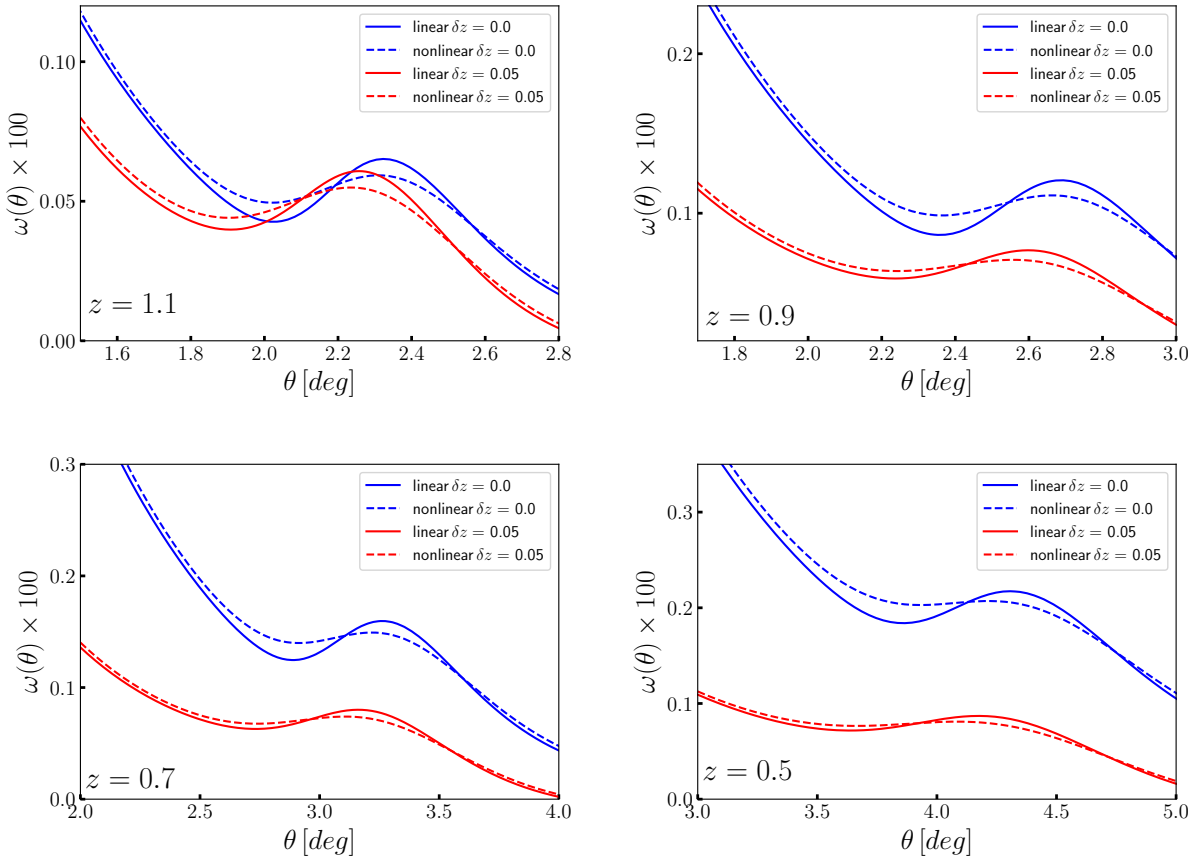

Figure 1. These four plots, at 4 redshifts $\bar{z} = 1.1, 0.9, 0.7, 0.5$, illustrate the linear and nonlinear evolution of the matter clustering with BAO signature at different epochs of the Universe. We also show, in each panel, a comparison of how this signal behaves in the 2PACF considering two cases for the size of the redshift bin, δz. The shift in the BAO signal position in the $\delta z \neq 0$ case, with respect to the $\delta z = 0$ case, determines the shift correction to be added to $\theta_{\rm FIT}$, the value achieved fitting the 2PACF with a BAO bump signature: $\theta_{\rm BAO}(\bar{z}) = \theta_{\rm FIT}(\bar{z})\,[1 + \Delta(\bar{z}, \delta z)]$.

3. Final remarks

The measurement of the radial and angular BAO scales at several redshifts is of fundamental importance if one aspires to know the dynamics of the Universe.

To perform transversal BAO measurements in redshift shells of data one has to consider the projection effect [28,29]. The difference in the BAO signal position in the $\delta z \neq 0$ case, with respect to the $\delta z = 0$ case, determines the shift correction to be added to the value $\theta_{\rm FIT}$ obtained fitting the 2PACF with a BAO bump signature: $\theta_{\rm BAO}(\bar{z}) = \theta_{\rm FIT}(\bar{z})\,[1 + \Delta(\bar{z}, \delta z)]$.

As observed in Table 1 where we consider redshift shells of width $\delta z = 0.05$, the cosmological model dependence of the BAO measurement is actually weak and quantifiable [38,39]. For thinner redshift bins, $\delta z \to 0$, the shift due to the projection effect is smaller, therefore the model dependence is weaker. Moreover, in many cases, this correction is smaller than other errors, like statistical error, that also contribute to the final error of the BAO measurement.

Acknowledgments

EdC acknowledges the PROPG-CAPES/FAPEAM program. AB and JCC acknowledge the support of the Brazilian agency CNPq. We also thank the CAPES PVE project 88881.064966/2014-01, within the *Science without Borders Program*.

[1] York D G et al. 2000 *Astron. J.* **120** 1579 (*Preprint* arXiv:astro-ph/0006396)
[2] Planck Collaboration (Planck 2013 results. I.) 2014 *Astron. & Astrophys.* **571** A1 (*Preprint* arXiv:1303.5062)
[3] Bertini N R, Hipolito-Ricaldi W S, Santos F dM, Rodrigues D C 2019 (*Preprint* arXiv:1908.03960)
[4] Herrera R, Hipolito-Ricaldi W S, Videla N 2016 *JCAP* **08** 065 (*Preprint* arXiv:1607.01806)
[5] Hipolito-Ricaldi W S, Brandenberger R, Ferreira E G M, Graef L 2016 *JCAP* **11** 024 (*Preprint* arXiv:1605.04670)
[6] Romero Fuño A, Hipolito-Ricaldi W S, Zimdahl W 2016 *MNRAS* **457** 2958 (*Preprint* arXiv:1409.7706)
[7] Zuñiga Vargas C, Hipolito-Ricaldi W S, Zimdahl W 2012 *JCAP* **04** 032 (*Preprint* arXiv:1112.5337)
[8] Zimdahl W et al. 2011 *JCAP* **04** 028 (*Preprint* arXiv:1009.0672)
[9] Hipolito-Ricaldi W S, Velten H E S, Zimdahl W 2009 *JCAP* **06** 016 (*Preprint* arXiv:0902.4710)
[10] Bernui A, Hipolito-Ricaldi W S 2008 *MNRAS* **389** 1453 (*Preprint* arXiv:0807.1076)
[11] Kumar S, Nunes R C, Kumar Yadav S 2018 *Phys. Rev.* D **98** 2018 043521 (*Preprint* arXiv:1803.10229)
[12] Nunes R C 2018 *JCAP* **05** 052 (*Preprint* arXiv:1802.02281)
[13] Ghosh S et al. 2016 *J. Astrophys. Astron.* **37** 25 (*Preprint* arXiv:1610.08176)
[14] Bernui A, Ferreira I S, Wuensche C A 2008 *Astrophys. J.* **673** 968 (*Preprint* arXiv:0710.1695)
[15] Bengaly C A P, Bernui A, Alcaniz J S, Ferreira I S 2017 *MNRAS* **466** 2799 (*Preprint* arXiv:1511.09414)
[16] Bengaly C A P et al. 2018 *MNRAS* **475** L106 (*Preprint* arXiv:1707.08091)
[17] Marques G A, Novaes C P, Bernui A, Ferreira I S 2018 *MNRAS* **473** 165 (*Preprint* arXiv:1708.09793)
[18] Planck Collaboration (Planck 2013 results. XXIII.) 2014 *Astron. & Astrophys.* **571** A23 (*Preprint* arXiv:1303.5083)
[19] Novaes C P, Bernui A, Marques G A, Ferreira I S 2016 *MNRAS* **461** 1363 (*Preprint* arXiv:1606.04075)
[20] Bernui A 2009 *Phys. Rev.* D **80** 123010 (*Preprint* arXiv:0912.1147)
[21] Gruppuso A et al. 2013 *JCAP* **07** 047 (*Preprint* arXiv:1304.5493)
[22] Gruppuso A 2014 *MNRAS* **437** 2076 (*Preprint* arXiv:1310.2822)
[23] Bernui A, Novaes C P, Pereira T S, Starkman G D 2018 (*Preprint* arXiv:1809.05924)
[24] Aluri P K, Ralston J P, Weltman A 2017 *MNRAS* **472** 2410 (*Preprint* arXiv:1703.07070)
[25] Planck Collaboration (Planck 2013 results. XXIV.) 2014 *Astron. & Astrophys.* **571** A24 (*Preprint* arXiv:1303.5084)
[26] Bernui A, Tsallis C, Villela T 2006 *Phys. Lett.* A *356* 426 (*Preprint* astro-ph/0512267)
[27] Bernui A, Rebouças M J 2012 *Phys.Rev.* D **85** 023522 (*Preprint* arXiv:1109.6086)
[28] Bernui A, Mota B, Rebouças M J, Tavakol R 2007 *Int. J. Mod. Phys.* D **16** 411 (*Preprint* arXiv:0706.0575)
[29] Aluri P K, Rath P K 2016 *MNRAS* **458** 4269 (*Preprint* arXiv:1202.2678)
[30] Novaes C P et al. 2014 *JCAP* **01** 018 (*Preprint* arXiv:1312.3293)
[31] Novaes C P et al. 2015 *JCAP* **09** 064 (*Preprint* arXiv:1409.3876)
[32] Avila F, Novaes C P, Bernui A, de Carvalho E 2018 *JCAP* **12** 041 (*Preprint* arXiv:1806.04541)
[33] Avila F, Novaes C P, Bernui A, de Carvalho E, Nogueira-Cavalcante J P 2019 *MNRAS* **488** 1481 (*Preprint* arXiv:1906.10744)
[34] Laurent P et al. 2016 *JCAP* **11** 060 (*Preprint* arXiv:1602.09010)
[35] Eisenstein D J et al. (SDSS Collaboration) 2005 *Astrophys. J.* **633** 560 (*Preprint* arXiv:astro-ph/0501171)
[36] Peebles P J E, Hauser M G 1974 *Astrophys. J. Suppl.* **28** 19
[37] Landy S D, Szalay A S 1993 *Astrophys. J.* **412** 64
[38] Sánchez E et al. 2011 *MNRAS* **411** 277 (*Preprint* arXiv:1006.3226)
[39] de Carvalho E et al. 2018 *JCAP* **04** 064 (*Preprint* arXiv:1709.00113)
[40] Novaes C P et al. 2018 *MNRAS* **478** 3253 (*Preprint* arXiv:1805.04078)
[41] Marques G A et al. 2019 *JCAP* **06** 019 (*Preprint* arXiv:1812.08206)
[42] Marques G A, Bernui A 2019 (*Preprint* arXiv:1908.04854)
[43] Planck Collaboration (Planck 2018 results. VI.) 2019 (*Preprint* arXiv:1807.06209)